SHEAR STRENGTH OF THERMALLY SPRAYED COATINGS

MICHAELA KAŠPAROVÁ, JOSEF VOLÁK, FRANTIŠEK ZAHÁLKA, and ŠÁRKA HOUDKOVÁ

ŠKODA VÝZKUM Ltd., Tylova 1/57, 316 00 Plzeň, Czech Republic
michaela.kasparova@skodavyzkum.cz

Keywords: shear strength, thermally sprayed coatings, cohesion, adhesion

1. Introduction

The test of tensile adhesive strength of thermally sprayed coatings is commonly used method but it has some limits namely the necessity of samples bonding using adhesive or glues with high tensile strength. In the dependency on the coating chemical composition and microstructure, the values of the bond strength can be artificial improved due to adhesive penetration in coating porosity and formation the chemical compounds. These negative effects can be eliminated using the shear tests without adhesives. These tests are closer to real situation than tensile bond strength test. Several methods and systems arrangement for shear loading were designed and described e.g. in ref.[1–3]. The shear test according to EN 15340 is the most commonly used test for measuring the shear strength of coatings. Other methods e.g. in ref.[5,6] are described (punch test, indentation test, pre-notched four-point bending test, non-destructive methods). The main purpose of the shear tests is to determine the resistance against shear loading on the coating-substrate interface (adhesive strength) or the strength of the coating itself (cohesive strength).

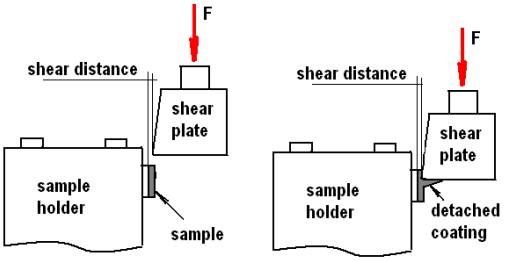

Fig. 1. **Principle of the shear test**

The purpose of this study was to modify the shear coating strength test in accordance with ČSN EN 15340 Standard, where the coating is uniformly loaded in parallel to the coating/substrate interface. The principle of the test is depicted in Fig. 1. With respect to the substrate roughness, the shear distance must be 50 μm ± 20 μm from the substrate. Lyphout et al.[4] evaluated the influence of the shear distance on the shear strength of the coating. They mentioned increasing of shear strength by about 45 MPa when the shear distance was 140 μm comparing to the shear distance of 60 μm.

During the shear tests the coating is loaded with smooth moving of the shear tool at a constant velocity till fracture occurs and the load drops down. The first maximum of the load curve defines the resistance to the shear stress.

2. Experiment

2.1. Samples preparation

The commercially available (15–45 μm) Triballoy 400 (CoMoCrSi), Stellite Alloy 6 (CoCrWCSi) and 13 % Cr were deposited on low-carbon steel substrates of 40×50×30 mm in size. Trib400 and Stellite were prepared using the JP-5000 HP/HVOF technology and 13 % Cr using the arc spray technology. The substrates were cleaned by grit-blasting with (0,8–1 mm) brown corundum. The TTN 24 Sand Blaster was used, the blasting distance was 12 cm and the blasted pressure was 6 atm. The substrate roughness was R_a = 9 μm. The coatings were sprayed using the optimized spray parameters. The final coatings thickness was 500 ± 50 μm for all sprayed samples. After spraying, the samples were cut for the shear test by the water jet to the size of 5×10×30 mm.

2.2. Experimental measurements

The shear strength of coatings was measured in accordance with ČSN EN 15340 Standard. The coating located on one facing surface of the tested sample was loaded with the compression stress by the loading velocity of 50 μm s^{-1}. The sample fixing was ensured using two screws in the special tool, which prevents sample movement in all directions. The microstructure was investigated using scanning and light microscope on the coatings cross sections.

3. Results and discussion

Typical shear curves for the tested samples are shown in Fig. 2. The shear force of Stellite coating was 1900 MPa and that of Triballoy400 was 1945 MPa, while the shear strength of arc sprayed 13 % Cr coating was lower, 1500 MPa. Seven measurements for each coating were performed. Average values of the shear test are mentioned in Tab. I. The shear strength of the HVOF coatings compared to the arc technology is higher due to homogenous, compact and dense structure with low content of oxides and un-melted particles, see Fig. 2. The fracture appearance in the coatings after the shear test is also documented in Fig. 3. It is evident that both HVOF coatings were fractured adhesively or adhesively-cohesively. It means that the coating was either fully detached from the substrate the crack propagated inside the coating. In the case of 13 % Cr coating, the elastic behaviour was found, see

Table I
Summary of the shear tests

Coating	Shear force F_{max} [N]	Shear strength σ_{max} [MPa]	Failure
Stellite	1900±180	38±3.6	a-c
Trib 400	1945±166	39±3.3	a-c
13%Cr	1350±140	27±2.8	a-c

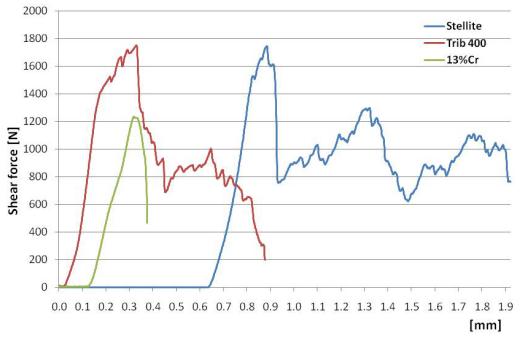

Fig. 2. **Record of the shear curves**
*shear modes definitions are stated in ČSN EN 15340 Standard

Fig. 2, because only the coating deflection for all tested samples occurred after the coating detaching.

Different failure modes can be observed during the shear test. They are caused by different modes of crack propagation in the coating during the shear stress action*. The different crack types are influenced by the coating material, adhesion properties between substrate and coating and the cohesion properties between the coating phases. The curves for the HVOF coatings were mostly in mode 2, which means that the coating adhesion is higher than its cohesion. In failure of mode 3, the coating is separated into small parts by the shear plate from the ground material. This behavior is typical for coatings with high hardness. However, the failure mode 1 was also observed for those coatings (the coatings detach along the whole coating-substrate interface). For the 13 % Cr coating, only the failure in mode 3b was observed, which means that the coating separate in large parts by the shear plates.

4. Conclusion

The shear test used for the evaluation of the shear strength of thermally sprayed coatings is convenient method for fast, easy and objective investigation of one of the coating parameters that relates to the coating strength properties and lifetime. The HVOF coatings exhibit higher shear strength compared to arc coatings due to more compact and denser microstructure and higher bond strength to the base material. It was achieved by high impact velocity and kinetic energy of impinging particles on the substrate.

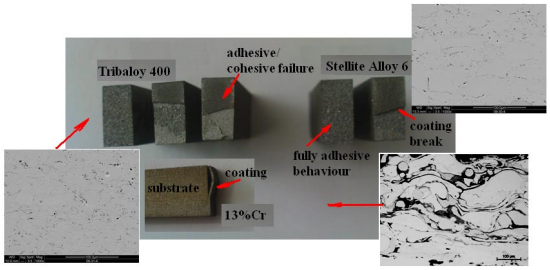

Fig. 3. **Documentation of coating fracture after the shear test**

This work was supported by the project No. VZ/MSM 4771868401.

REFERENCES

1. Callus P. J., Berndt C. C.: *Proceedings of 12th International Thermal Spray Conference, London*, UK (1989) 69 -76.
2. Era H., Otsubo F., Uchida T., Fukuda S., Kishitake K.: J. Mater. Sci. Eng. *A251*, 166 (1998).
3. Grutzner H., Dvorak M., Siegmann S., Nassentstein K.: *ITSC 2004 Thermal Spray Solutions – Advances in Technology and Applications*, Osaka, Japan, DVS, (2004), p. 364–368.
4. Lyphout C., Nylén P., Wigren J.: *Char. of Adhesion Strength and residual Stresse of HVOF sprayed Inconel 71/ for Aerospace Repair Applications*, ITSC 2007, p. 588–593.
5. Sakata K. et al.: *Effect of diffusion treatment on the interface microstructure between ts cobalt-based self-fluxing alloy coating and steel substrate*, ITSC 2008, p.696–700.
6. Ducos M., Bossuat B., Walesyek H., Canal B.: *Non-destructive testing of the coating-substrate interface of thermally-sprayed industrial parts*, ITSC (2005) p. 1041 –1046.

M. Kašparová, J. Volák, F. Zahálka, and Š. Houdková *(ŠKODA VÝZKUM Ltd., Plzeň, Czech Republic)*: **Shear Strength of Thermally Sprayed Coatings**

HVOF-coatings of Stellit Alloy 6 and Trib400 and the arc-coating of 13 % Cr were investigated using shear tests in accordance with EN 15340 Standard. The shear curves and the maximal shear forces were recorded and compared with each other. Also the fracture appearance after the tensile tests was documented using scanning electron microscopy. The results give beneficial information about adhesive-cohesive behaviour of thermally sprayed coatings which facilitate to predicate mainly the shear, impact resistance and coatings lifetime.

INFLUENCE OF TEMPERATURE ON MICROHARDNESS OF ALUMINIUM-BASED COMPOSITES PRODUCED BY CONTROLLED HYPEREUTECTIC REACTION IN Al-Ni BINARY SYSTEM

LENKA KLAKURKOVÁ[a,*], LADISLAV ČELKO[a], KAREL SLÁMEČKA[b], PAVEL DOLEŽAL[a], and JIŘÍ ŠVEJCAR[a]

[a] Institute of Materials Science and Engineering, [b] Institute of Physical Engineering, Faculty of Mechanical Engineering, Brno University of Technology, Technická 2896/2, 616 69 Brno, Czech Republic
klakurkova@fme.vutbr.cz

Keywords: Al-rich intermetallics, aluminium-based composites, hypereutectic alloys, microhardness

1. Introduction

In the Ni–Al binary system, the majority of scientific attention is focused on the development of NiAl and Ni_3Al phases. The Ni–Al binary system also contains other three, less known phases. The $NiAl_3$, Ni_2Al_3 and Ni_5Al_3 phases are not considered for use in high-temperature applications mainly due to their lower melting points being 854 °C, 1133 °C and approx. 700 °C, respectively[1–4]. New information about their formation and degradation mechanisms, morphology, and distribution, physical and mechanical properties can be, however, successfully used for strengthening of Al composites, Ni/Al/Ni interconnections, and layered structures design[5,6].

This contribution is focused on local mechanical properties represented by microhardness of Al substrate and strengthening Al-rich intermetallic phases produced from deposited Ni sacrificial coatings after the annealing in a wide range of temperatures encompassing the solid and/or molten state of the aluminium substrate.

2. Experimental

Aluminium sheet of commercial purity (99.5 wt.%) was used as a substrate. A commercially available nickel (99.7 wt.%) powder was deposited onto the substrate using High Velocity OxyFuel technique. The thickness of deposited coating was in the range of 250–300 μm. Subsequent annealing in the temperature ranges 600–630 °C (solid state), 640–660 °C (semi-solid state) and above 660 °C (liquid state of aluminium) with appropriate dwells was applied regarding to Al-rich aluminides Ni_2Al_9, $NiAl_3$ and Ni_2Al_3 formation at the coating-substrate interface and/or at the aluminium substrate.

The resulting microstructures were obtained by scanning electron microscopes (JEOL-840A, Philips XL-30). Local mechanical properties, represented by microhardness of the aluminium substrate and intermetallics formed, after the annealing was measured by the microhardness tester (LECO LM 247AT).

3. Results

At the temperatures below the Al + $NiAl_3$ eutectic melting point (639.9 °C), aluminium from the substrate diffuse primarily toward the coating and forms the $NiAl_3$ and Ni_2Al_3 layers, see Figs. 1a and 1b. In dependence on the temperature heigh the different annealing times were used to their formation. Their thicknesses increase markedly faster at higher temperatures applied. Nickel diffuse from the rating into the substrate and form $NiAl_3$ and/or Ni_2Al_9 intermetallic particles. These take up only 2.5 vol.% at maximum.

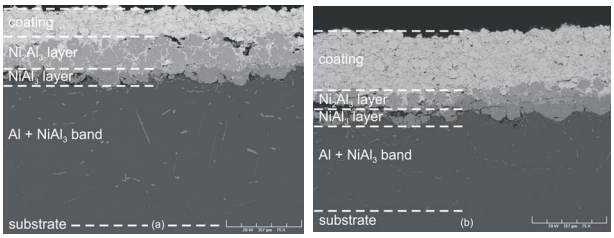

Fig. 1. **Coating-substrate interface after annealing (a) 600 °C / 500 hrs, (b) 630 °C / 50 hrs – SEM-BSE**

In the range of 640–660 °C, the onset of liquid aluminium phase can be expected. The nickel coating dissolves in aluminium substrate. Total thickness of the original coating deposited onto the substrate decreases during annealing. Discontinuous Ni_2Al_3 and $NiAl_3$ layers start to form at these interfaces, see Figs. 2a and 2b. The region denoted as Al + $NiAl_3$ band consists of Al + $NiAl_3$ eutectic and primary $NiAl_3$ particles. Strengthening phases formed in the substrate occupy 20 vol.%. Below 645 °C, the Al + $NiAl_3$ eutectic was never observed, see the system at lower temperatures.

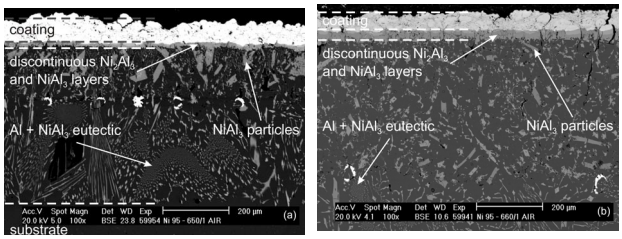

Fig. 2. **Coating-substrate interface after annealing (a) 650 °C / 60 min, (b) 660 °C / 60 min – SEM-BSE**

At temperatures exceeding 660 °C, the Al substrate is completely in the liquid state. The dimensions of Al substrate body do not change dramatically, because of the existence of oxide cover which keeps the substrate compact. In the first minutes of annealing the coating is almost or completely dis-

solved in the substrate, see Figs. 3a and 3b. At the temperatures higher than 800 °C, significantly higher amount of $NiAl_3$ particles was formed. The growth rate of eutectic band thickness could be also governed by dwell time at annealing temperature. The strengthening phases occupy up to 35 vol.% of the substrate on average.

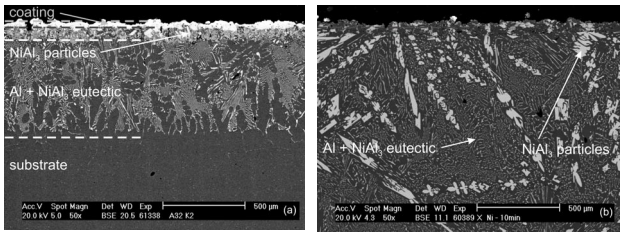

Fig. 3. **Coating-substrate interface after annealing (a) 700 °C / 10 min, (b) 800 °C / 10 min – SEM-BSE**

Measured and averaged values of microhardness of selected structural parts are presented in Fig. 4. Significant drop in hardness of primary $NiAl_3$ particles down to the range of 600–650 HV is observed at temperatures of 650 and 700 °C. The drop of microhardness within this range can result from contribution of the substrate iron-based impurities, which participates on the primary $NiAl_3$ stoichiometric compound formation. At the same temperatures finer morphology of Al + $NiAl_3$ eutectic formation was observed. Above the 650 °C, where the Al + $NiAl_3$ eutectic region starts to form, the hardness 75 HV remains stable. The aluminium substrate harndess of about 40 HV was measured with increasing temperature of the Al-Ni hypereutectic composite formation.

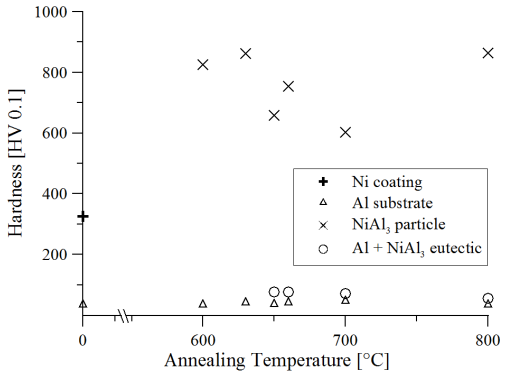

Fig. 4. **Hardness of selected structural parts**

The composite hypereutectic alloy prepared from sacrificial nickel coatings at the temperature of 700 °C seems to be the most interested choice because of the formation of finer Al + $NiAl_3$ eutectic.

4. Conclusions

- The hardness of primary $NiAl_3$ phase change markedly at the temperatures of 650 and 700 °C.
- The optimal condition for processing of Al–Ni composites from sacrificial coatings is at the temperature of 700 °C.
- To form the layered structures containing Al-rich intermetallics, the temperatures below the eutectic melting point can be used.
- The origin of layers and/or composite, are diffusion-driven and can be governed by the annealing dwell.

This work was financially supported by the Czech Science Foundation Project No. 106/09/P513.

REFERENCES

1. Morsi K.: Mat. Sci. Eng. A *299*, 1 (2001).
2. Tamarin Y.: *Protective Coatings for Turbine Blades*. ASM International, Ohio 2002.
3. Čelko L., Klakurková L., Man O., Švejcar J.: Mater. Manuf. Proc. *24*, 1155 (2009).
4. Garg S. P., Kale G. B., Patil R. V., Kundu T.: Intermetallics *7*, 901 (1999).
5. Gonzalez G., Lara-Rodriguez G. A., Sandoval-Jimenéz A., Saikaly W., Charai A.: Mater. Char. *59*, 1607 (2008).
6. Čelko L., Klakurková L., Švejcar J.: Def. Diff. Forum. *297-301*, 771 (2010).

L. Klakurková[a], L. Čelko[a], K. Slámečka[b], P. Doležal[a], and J. Švejcar[a] *([a] Institute of Materials Science and Engineering, [b] Institute of Physical Engineering, Faculty of Mechanical Engineering, Brno University of Technology, Brno, Czech Republic):* **Influence of Temperature on Microhardness of Aluminium-Based Composites Produced by Controlled Hypereutectic Reaction in Al-Ni Binary System**

Aluminium matrix composites were prepared by High Velocity OxyFuel spraying of nickel powder onto the aluminium sheet's surface followed by annealing in a range of temperatures 600–630 °C (solid state), 640–660 °C (semi-solid state) and above 660 °C (liquid state of aluminium). The Ni_2Al_3 and Ni Al_3 intermetallic layers were formed at the interface between original Ni coating and Al matrix. Moreover, Ni diffused into the aluminium matrix and caused strengthening of $NiAl_3$ and Ni_2Al_9 particles. Local mechanical properties represented by microhardness of aluminium matrix and intermetallic phases formed were measured.

INFLUENCE OF DEFORMATION DEGREE ON LOCAL DEFORMATION HETEROGENEITY DURING THIN SHEET ROLLING

RÓBERT KOČIŠKO[a], JÚLIUS BACSÓ[a], JANA BIDULSKÁ[a*], ANDREA KOVÁČOVÁ[a], PETER BELLA[a], and MÁRIA MOLNÁROVÁ[b]

[a] Department of Metals Forming, Faculty of Metallurgy, Technical University of Košice, 042 00, Košice, [b] Institute of materials research, Slovak Academy of Sciences, 040 01, Košice, Slovakia
jana.bidulska@tuke.sk

Keywords: FEM, cold rolling, deformation heterogeneity

1. Introduction

The non-uniform deformation is always being formed throughout deformation band volume during rolling process[1,2]. The non-uniform deformation reduces the strain of core parts contributing to structural non-homogeneity through the thickness of sheet such as non-uniform grain size, anisotropy, etc. These aspects also contribute to the structural non-homogeneity through sheet thickness such as non-uniform grain diameter, and the anisotropy. On the other hand, non-uniform deformation through the thickness of thin sheet represents the different energy areas resulting in the development of the recovery processes in the further processing. It is possible to achieve precisely defined deformation non-homogeneity through the thin sheet thickness by means of the controlled rolling.

Geometric ratio l_d/h_s (l_d – length of contact arc, h_s – medium thickness of the sample) has the greatest impact on the distribution of deformation through thickness of semi-product. When l_d/h_s ratio is low, influence of rigid ends (the rolling of thick plates) has preferential effect and the friction importance is relatively small. However, when l_d/h_s ratio is high frictional forces have significant impact. J. J. Tarnovskij divided rolling conditions based on l_d/h_s folow[3]:

I. $l_d/h_s < 0.2$ the compressive deformation is concentrated below the surface,
II. $0.15–0.2 < l_d/h_s < 0.6–0.7$ the compressive deformation penetrates to the core gradually,
III. $0.6–0.7 < l_d/h_s < 2–3$ the compressive deformation penetrates to the core gradually, following increase of spread in core parts leads to the formation of convex shape of the side walls,
IV. $l_d/h_s > 2–3$ the friction cones overlap together in the center part and thereby flow stress increases as well as convex shape of side walls.

The penetration of plastic deformation during thin sheets rolling can be also analysed using numerical simulations based on finite element method (FEM). Although the basic theoretical relationships between geometric ratio and penetration of plastic deformation are well known only few works have verified them or extended the theory on the impact of friction. FEM was used for: determining the distribution of rolling pressure along the strip width[4], the mathematical simulation of elastic entry and existence of regions in a roll bite zone[5], the study of a hot rolling process, the approach is based on thermo-mechanical analysis[6], the study of cold rolling of thin sheet with different friction conditions[7], determining the on-line accurate mean value of both friction coefficient and flow stress for anisotropic materials during cold rolling[8].
The aim of this study is to find out local penetration of plastic deformation during thin sheet rolling using FEM. The degree of plastic deformation and contact friction are variable parameters.

2. Experimental procedure

Rolling process of thin sheet was simulated using the software product Deform. The treshold conditions were defined by laboratory experiment[9]. The working rolls with diameter D = 210 mm were defined as a perfectly rigid body. The rotational speed of rolls was 8 rad, what is the rolling speed 0.83 m s^{-1}. The finite element mesh had 11850 node number for sample with input thickness h = 1.5 mm and length l = 50 mm. Number of elements through sample thickness was 25. The sample was defined as a plastic material. The experimental material is characterized as the C-Mn-Si steel. Flow stress is defined by equation $\bar{\sigma} = \bar{\sigma}(\bar{\varepsilon}, \dot{\varepsilon}, T)$, where $\bar{\sigma}$ is flow stress, $\bar{\varepsilon}$ is effective plastic strain, $\dot{\varepsilon}$ is effective strain rate, T is temperature. The average yield stress is 202 MPa. The elastic properties of samples are defined by Poisson's ratio 0.3 and Young's modulus 2.1×10^5 MPa.

The calculations of thin sheet rolling process were carried out by using different degrees of deformation 2 %, 4 %, 6 %, 8 % and 10 %. Three values of the contact friction coefficient f = 0.1; 0.6 and 0.9 were applied for all degrees of deformation.

3. Results and discussion

The amount of non-uniform deformation during process of thin sheet rolling is mostly influenced by geometric ratio l_d/h_s as well as friction coefficient. The change of geometric ratio for rolls diameter D = 210 mm was guaranteed by amount of the reduction (h). When degree of deformation is 2, 4, 6, 8, 10 %, l_d/h_s ratio is in the range 1.2–2.8 mm that falls into two areas based on Tarnovskij model. Fig. 1 shows the effective strain in dependence on degree of plastic deformation and change of contact friction. Distribution of effective strain was analysed through sample thickness. The highest effective strain intensity was below the surface (about 20 % of the total thickness of the plate) and decreases towards the core of the sheet gradually. The deformation degree had negligible influence on the effective strain heterogeneity between samples surface and core (Δφ). Distribution of effective deformation through material thickness calculated by mathematical simulations was

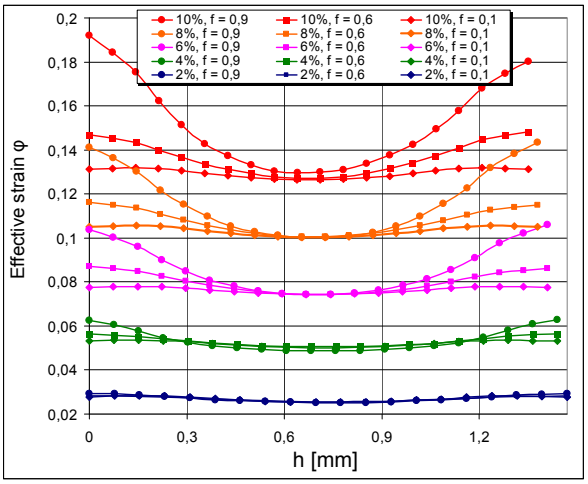

Fig. 1. **Effective strain in dependence on the degree of deformation and contact friction level**

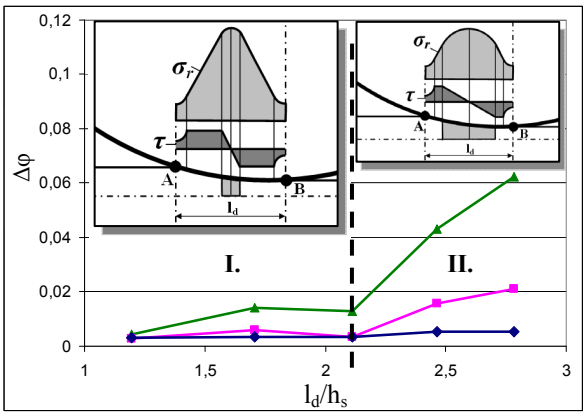

Fig. 2. **Effective strain between samples surface and core (Δφ). depending on l_d/h_s and the contact friction**

confirmed by experimental microhardness measurements presented by authors[9].

The contact friction coefficient for different geometric ratios l_d/h_s had influence on the Δφ more significantly, as seen in Fig. 2. The dependence in terms of friction is possible to divide into two areas:

I. $l_d/h_s < 2.1$ – in this area the friction has negligible influence on Δφ, band adhesion is concentrated only in narrow range around the neutral plane along l_d, substantial part of l_d is formed by band slip. Moreover, backward slip zone and forward slip zone are also observed.

II. $l_d/h_s > 2.1$ – in this area friction has significant influence on Δφ, adhesion band makes main part of l_d, slip band is being minimized while backward slip zone and forward slip zone are preserved.

4. Conclusion

When friction is low (f = 0.1), l_d/h_s ratio has negligible influence on the plastic deformation heterogeneity during thin sheet rolling. Significant influence of contact friction appears when $f > 0.6$ at $l_d/h_s > 2.1$. These threshold values cause extension of adhesion zone along l_d and resulting in the enhancement of non-uniform effective strain between the center and edge of the sheet.

This work was realized within the frame of the project „Technological preparation of electrotechnical steels with high permeability for electrodrives with higher efficiency“, which is supported by the Operational Program “Research and Development” ITMS 26220220037, financed through European Regional Development Fund.

REFERENCES

1. Zamyslovský Z.: Hutnícke listy *2*, 101 (1971).
2. Kvačkaj T.: Neue hütte *6/7–92*, 225 (1992).
3. Kollerová M., Žídek M., Dědek V., Počta B.: *Valcovanie*, Alfa, Bratislava 1991.
4. Liu X., Shi X., Li S., Xu J., Wang G.: J. Iron Steel Res. Int. *14*, 22 (2007).
5. Jiang Z. Y., Tieu A. K., Lu C.: J. Mater. Process. Technol. *146*, 167 (2004).
6. Galantuccia L. M., Tricarico L.: J. Mater. Process. Technol. *92–93*, 494 (1999).
7. Jiang Z. Y., Tieu A. K.: Tribol. Int. *37*, 185 (2004).
8. Han H.: J. Mater. Process. Technol. *159*, 401 (2005).
9. Gavendová P., Kováč F., Stoyka V., Petryshynets I., Kvačkaj T.: Acta Metallurgica Slovaca *16*, 181 (2010).

R. Kočiško[a], J. Bacsó[a], J. Bidulská[a], A. Kováčová[a], P. Bella[a], and M. Molnárová[b] *([a] Department of Metals Forming, Faculty of Metallurgy, Technical University of Košice, [b] Institute of materials research, Slovak Academy of Sciences, Košice, Slovakia):* **Influence of Deformation Degree on Local Deformation Heterogeneity During Thin Sheet Rolling**

The cold rolling process of thin sheet was simulated by a two-dimensional rigid-plastic finite element method (FEM) to find out local penetration of plastic deformation during thin sheet rolling. It was found of that the deformation degree had negligible influence on the effective strain heterogeneity between surface and core samples (Δφ) in dependence on the degree of plastic deformation and contact friction. The contact friction coefficient for different geometric ratios l_d/h_s influenced Δφ more significantly.

INDENTATION THERMAL SHOCK RESISTANCE OF Si_3N_4/CNT COMPOSITES

ALEXANDRA KOVALČÍKOVÁ[a]*, TAPASZTÓ ORSOLYA[b], CSABA BALÁZSI[b], and JÁN DUSZA[a]

[a] *Institute of Materials Research, Slovak Academy of Sciences, Watsonova 47, 040 01 Košice, Slovak Republic,* [b] *Ceramics and Composites Laboratory, Research Institute for Technical Physics and Materials Science, Hungarian Academy of Science, Konkoly-Thege ut 29-33, 1121 Budapest, Hungary*
akovalcikova@imr.saske.sk

Keywords: Si_3N_4/CNT composites, indentation thermal shock resistance, crack propagation

1. Introduction

Carbon nanotubes (CNTs) offer new possibilities to improve the functional and mechanical properties of advanced ceramics thanks to their small diameter, large aspect ratio, low mass and excellent mechanical, electrical and thermal properties[1]. During the last decade new ceramic/carbon nanotube composites have been developed and a number of authors have reported improved mechanical and functional properties in the case of ceramic/CNT composites compared to the monolithic material[2]. Three main problems have been recognized during these investigations: dispersion of the CNTs in the matrix, densification of the composites and degradation of the CNTs.

However, only few researchers have been concerned with thermal properties of carbon nanotube composites in ceramic systems. In convectional testing thermal shock resistance (TSR) is quantified by measuring of residual strength of polished specimens after quenching. This standardized method requires a large number of prepared samples, it cannot allow multiple shock measurements. For these reasons an alternative indentation-quench method has been developed[3]. In this technique, the TSR is measured by studying the propagation of median/radial cracks around a Vickers indentation after single or repeated quenching. The critical temperature difference DTc, of the material can be defined with reference to the number of propagating cracks and the amount of crack extension.

The main aim of this study is an estimation of indentation TSR of Si_3N_4/CNT composites.

2. Experimental procedure and materials

Si_3N_4, Al_2O_3 and Y_2O_3 were used as starting powders. Different amount of CNTs were added in addition to batches (1 and 3 wt.%). The powder mixtures together with the added CNTs were milled in ethanol for 3 h. The batches were dried and sieved. Green samples were obtained by dry pressing at 220 MPa. The samples without CNT were fabricated in the same manner. HIP was performed at 1700 °C in high purity nitrogen at gas pressure 20 MPa.

For the investigation of TSR the indentation-quench method was used. The length of the cracks was measured using optical microscopy. After the indentation the samples were heated in a vertical tube furnace in air to the required temperature and held there for 25 min. Then the specimens were rapidly immersed into a ~20 °C water bath. Final radial crack lengths were then measured with optical microscope. The procedure was repeated at increasing quenching temperatures ΔT, up to the critical value of ΔTc at which radial crack became unstable and the specimen failed.

3. Results

The microstructure of sintered CNT composites (Fig. 1) consisted mainly of β-Si_3N_4 grains (several micro meters in length) and nanotubes. The CNTs are located mainly in the inter-granular positions and they have a good contact to the surface of silicon nitride grains. The dispersion of nanotubes is still far from optimum, in most of the cases they are in interconnected groups.

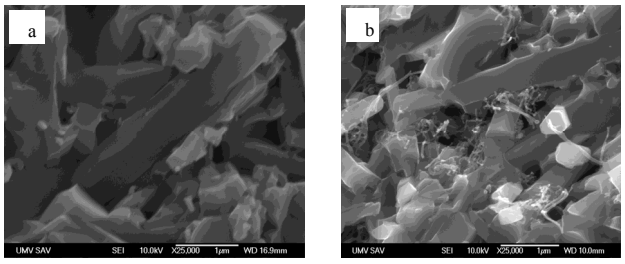

Fig. 1. **Fracture surfaces of HIP samples (a) Si_3N_4 reference sample, (b) CNT/Si_3N_4 composties with 3 % CNT**

The initial cracks size for silicon nitrides samples were ≈ 120 μm at indentation load 98.1 N. The dependence of radial crack growth on temperature for tested materials is plotted in Fig. 2. There are visible three different areas which characterize the crack evolution after quenching: a) an initial radial cracks growing slightly with increasing ΔT (area to ΔT ~ 200 °C); b) a radial crack growing stable extension (area ΔT 200–700 °C); c) a radial crack growing unstable extension and the specimens failed. A critical temperature ΔT_c when the Si_3N_4 failed is ~ 780 °C. In the case of Si_3N_4/CNT reinforced composites the initial crack length was above 125–130 μm. Again are visible different areas which characterize the crack evolution after quenching: a) an initial radial cracks growing slightly with increasing ΔT (area to ΔT ~ 250 °C for SN-CNT1, to ΔT ~ 200 °C for SN-CNT2); b) a radial crack growing stable extension (area ΔT 250–700 °C for SN-CNT1, ΔT 200–600 °C for SN-CNT2; c) a radial crack growing unstable extension and the specimens failed (ΔT_c~ 870 °C for SN-CNT1 and ΔT_c~ 620 °C for SN-CNT2).

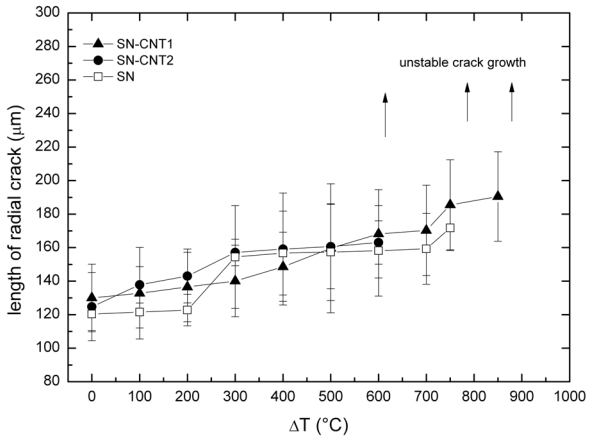

Fig. 2. **Crack propagation at thermal shock tests**

With increasing the CNT content a decrease of TSR has been observed. TSR can be improved by the increased flexural strength and fracture toughness and by decreased Young's modulus and coefficient of thermal expansion. Because fracture toughness for Si_3N_4/CNT (6.0 MPa $m^{1/2}$) does not differ significantly from the values of Si_3N_4 (6.3 MPa $m^{1/2}$), the reason for lower TSR could be degraded strength values by CNT dispersions due to insufficient densification[4]. The other possible reason is a difference in thermal properties of the materials- thermal expansion coefficients of Si_3N_4 (3.10^{-6} K^{-1}) and CNTs ($1.6–2.6.10^{-5}$ K^{-1}). Microfractographic observation of thermally shocked specimens with Vickers indentation showed well defined radial crack pattern. The propagation of Vickers indentation crack of SN-CNT1 before and after thermal shock at $\Delta T = 870$ °C is shown in Fig. 3. These cracks increased in size with increasing temperature, but always reached instability first in the longitudinal direction.This indicates a slightly higher tension in the transverse direction, consistent with some edge effect in the thermal transfer process (via r_0 in the Biot coefficient)[5].

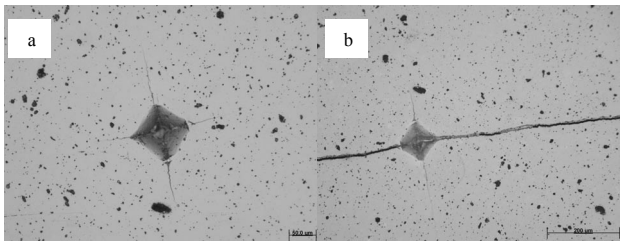

Fig. 3. **Vickers indentation crack of SN-CNT1, (a) before thermal shock, (b) after thermal shock (ΔT = 870 °C)**

4. Conclusion

With increasing the carbon nanotube content a decrease of thermal shock resistance has been observed. The reason for lower TSR could be degraded strength values by CNT dispersions due to insufficient densification and different thermal expansion coefficients of Si_3N_4 and CNTs.

This work was financed by the Slovak Government through the project LPP 0203-07 and by MNT-ERA.NET HANCOC.

REFERENCES

1. Merkoci A.: Microchim. Acta *152*, 157 (2006).
2. Tatami J., Katashima T., Komeya K., Meguro T., Wakihara T.: J. Am. Ceram. Soc. *88*, 2889 (2005).
3. Andersson T., Rowcliffe D. J.: J. Am. Ceram. Soc. *79*, 1509 (1996).
4. Balázsi Cs., Kónya Z.,Wéber F., Biró L. P., Arató P.: Mater. Sci. Eng. *C23*, 1133 (2003).
5. Lee S. K., Moretti J. D., Readey M. J., Lawn B. R.: J. Am. Ceram. Soc. *85*, 279 (2002).

A. Kovalčíková[a], T. Orsolya[b], Cs. Balázsi[b], and J. Dusza[a] *([a] Institute of Materials Research, Slovak Academy of Sciences, Košice, Slovak Republic, [b] Ceramics and Composites Laboratory, Research Institute for Technical Physics and Materials Science, Hungarian Academy of Science, Budapest, Hungary):* **Indentation Thermal Shock Resistance of Si_3N_4/ CNT Composites**

The influence of carbon nanotubes on the thermal shock resistance of the multiwall carbon nanotube reinforced silicon nitride composites has been investigated. Silicon nitride based composites with different amount (1 or 3 wt.%) of carbon nanotubes have been prepared by hot isostatic pressing. The adition of 1 wt.% CNTs enhanced the thermal shock resistance of the composite, however, CNT content increase up to 3 wt.% reduced its thermal shock resistance.

UNIVERSAL HARDNESS TEST APPLIED TO PM MATERIALS PREPARED FROM COATED POWDERS

MIRIAM KUPKOVÁ[a]*, MARTIN KUPKA[b], SUSANNE STROBL[c], and PAVOL HVIZDOŠ[a]

[a] Institute of Materials Research of SAS, Watsonova 47, Košice, [b] Institute of Experimental Physics of SAS, Watsonova 47, Košice, Slovakia, [c] Institute of Chemical Technology of Inorganic Materials, TU Vienna, Vienna, Austria
mkupkova@imr.saske.sk

Keywords: powder metallurgy, Cu-coated Fe powder, compaction, sintering, micromechanical properties

1. Introduction

Copper is an important alloying element in ferrous powder metallurgy (PM) due to its hardening effect (solid solution, precipitation) and for allowing the liquid phase sintering[1].

In order to distribute the alloying element uniformly, iron powder particles are often coated with a copper layer. The coating, in addition, removes the segregation of elements during transport and processing of the powders, it reduces harmful dustiness in the PM industry. The coatings also prevent powders from further oxidation, improve compressibility and enhance dimensional stability upon sintering.

To estimate the effective macroscopic properties of microheterogeneous materials, it is important to know the distribution, volume fractions and properties of individual phases constituting the material. However, the distinction of individual phases and determination of their mechanical properties is not straightforward and some indirect method has to be involved[2].

Nanoindentation has emerged as an important method for evaluation of the mechanical response of small material volumes to applied loading.

In the current investigation, nanoindentation tests are used extensively to determine the distribution of mechanical properties within the (sub)surface regions of the both "green" compacted and sintered cylinders prepared from Fe + 12 wt.% Cu coated powders.

2. Materials and experimental methods

Water-atomized iron powder, Höganäs ASC 100.29 grade, fraction 63−180 μm, was used as a starting raw material.

Iron particles were immersed into an aqueous electrolyte which contained coppersulfate and sulphuric acid. After stirring for several minutes, copper layer was deposited on surfaces of iron particles by cementation process. The required copper amount (12 wt.%) was controlled by the copper sulfate content in the electrolyte. More details on the fabrication and characteristics of the powders were presented elsewhere[1].

The powders obtained were cold-pressed into cylindrical compacts 10 mm in diameter and with heights of about 10 mm. The compaction pressure was 600 MPa. The lubricant was not added to the powder, zinc stearate was used as a die wall lubricant. Compacts were sintered in Marsch laboratory furnace at sintering temperature of 1120 °C for 60 minutes, in the atmosphere of 90 % N_2 – 10 % H_2.

To prepare for examinations, the samples were cut, mounted, ground, polished and nital-etched. The microstructure of the samples was analysed by a light optical microscope (OLYMPUS GX71, Japan).

The hardness and indentation elastic modulus were determined from the load-displacement curves, measured by the TTX-NHT apparatus with diamond Berkovich tip and analysed by the method developed by Oliver and Pharr[3]. The maximum load of 100 mN was chosen. The indentations were repeated twenty times for each sample. The irregular curves were excluded from analysis. Despite this, each thereinafter mentioned value represents an arithmetic average from at least 15 repeated measurements.

3. Results

At the temperature of 1120 °C, only about 8 wt.% of Cu may be dissolved in a solid iron. So, when the Fe + 12 wt.% Cu compact undergoes sintering at 1120 °C, the copper-rich liquid phase is permanently present. The melt penetrates into contacts between iron particles as well as along the grain boundaries into the interior of particles. This can cause particles to disintegrate. The disintegration leads to increased mobility of single grains and enables renewed (secondary) rearrangement.

As a result, the pore size, shape and distribution start to change. Pores are closing, spheroidizing and coalescing. Sintered compacts have thus got higher density (7.23 g cm^{-3}) than "green" ones (7.12 g cm^{-3}).

Simultaneously, the solid-state diffusion and solution-precipitation take place. The diffusion of copper into iron causes particles to become strengthened. This results in final sintered compacts consisting of hardened Fe particles bonded by a soft copper-based matrix.

Metallographic examination of the microstructure of compacted samples demonstrated that in "green" compacts the particle surfaces were almost completely covered with a copper (Fig. 1a). After sintering at the temperature of 1120 °C, the samples revealed a microgradient structure (Fig. 1b). After etching by nital, the Fe cores of original powder particles are less affected and the regions around, consisting of the Fe-Cu solid solution, are more attacked by the etching reagent (dark).

The changes in the mechanical properties are in close relation to these microstructures. Fig. 2 presents the average values of indentation hardness and indentation modulus. Pronounced differences in the indentation hardness and indentation modulus are observed for the "green" and sintered samples.

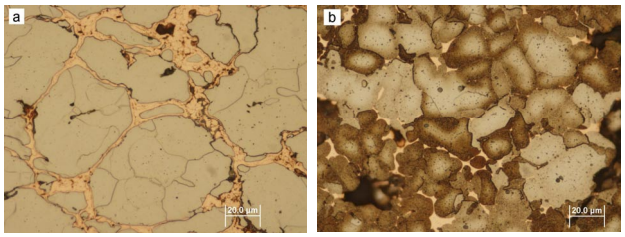

Fig. 1. **Structure of samples compacted at 600 MPa from iron powders coated with 12 wt.% of Cu. Sample in a "green" state (a) and (b) sintered at temperature 1120 °C and nital etched, LOM**

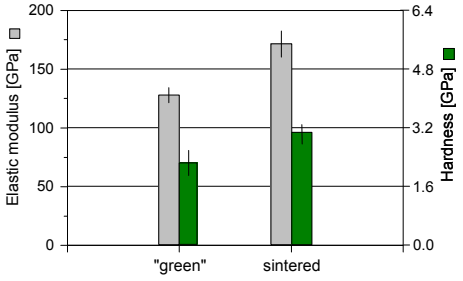

Fig. 2. **Indentation modulus and indentation hardness for samples prepared from 12 wt.% Cu coated iron powders**

The hardness and modulus are improved for sintered samples. They are strengthened by copper precipitation and by the formation of solid solution with iron.

4. Conclusion

In principle, the DSI method seems to be suitable for determining the "local" properties of PM samples.

Elastic properties are determined from the data obtained during unloading of the indentation. The indentation elastic modulus, E_{IT}, can be calculated from the slope of the upper portion of the unloading curve.

If the total measured compliance (the reciprocal of the slope of unloading curve) consists only of the compliance of contact between indenter and surface grain, the calculated elastic modulus corresponds to the Young's modulus E_m of the grain's material,

$$E_{IT} \approx E_m \qquad (1)$$

To allow for the "granular"character of the sample surface, we considered the total measured compliance as composed of two contributions – the compliance of the contact between indenter and the surface grain and the compliance of contact between the surface grain and the adjacent subsurface grain. Then we found that

$$E_{IT} \approx \frac{E_m}{1+2\left[\left(1+\frac{1-\nu_i^2}{1-\nu_m^2}\frac{E_m}{E_i}\right)\frac{r}{R}\right]^{1/3}} \qquad (2)$$

E_i and v_i are the Young's modulus and Poisson's ratio for the material of indenter; E_m and v_m are those for the grain's material. R is the radius of grain; r represents the radius of curvature of the indenter's tip.

The expression (*2*) shows that the indentation elastic modulus (i) does not exceed the modulus of grain's material, and (ii) should change with the size of grains. This change represents the goal of further investigations.

This work was supported by VEGA grant 2/0129/09 of the Slovak Grant Agency.

REFERENCES

1. Strobl S., Gierl C., Konnegger T., Kupková M., Kabátová M.: Powder Metall. Progress *6*, 149 (2006).
2. Němeček J., Lukeš J.: Chem. Listy *104*, 279 (2009).
3. Oliver W. C., Pharr G. M.: J. Mater. Res. *7*, 1546 (1992).

M. Kupková[a], M. Kupka[b], S. Strobl[c], and P. Hvizdoš[a]
([a] Institute of Materials Research of SAS, Košice, [b]Institute of Experimental Physics of SAS, Košice, Slovakia, [c] Institute of Chemical Technology of Inorganic Materials, TU, Vienna, Austria): **Universal Hardness Test Applied to PM Materials Prepared from Coated Powders**

Iron powder particles were coated with copper by cementation. The resultant powder contained 12 wt.% of copper. The coated powder was then compressed into cylindrical samples and sintered. Sintered samples possessed microgradient structure with a copper concentration decreasing from the surface towards the interior of iron grains. The hardness and elastic modulus of individual grains in both "green" and sintered samples were determined by the depth sensitive indentation method. The properties of sintered samples were found better than those of the "green" ones. To estimate the effect of "granular" structure of samples on measured properties, the relation for an indentation modulus based on a simple model was proposed.

IMPROVEMENT OF MECHANICAL PROPERTIES OF TPE BY IRRADIATION

MIROSLAV MAŇAS*, DAVID MAŇAS, MICHAL STANĚK, ŠTEPÁN ŠANDA, and VLADIMÍR PATA

Tomas Bata University in Zlin, nam. T.G.Masaryka 5555, 760 01 Zlin, Czech Republic
dmanas@ft.utb.cz

Keywords: thermoplastic elastomer, irradiation, mechanical properties

1. Introduction

The cross-linking of rubbers and thermoplastic polymers is a well-proven process of the improvement of the thermal properties. The chemical cross-linking or rubber vulcanization is normally induced by the effect of heating after processing with the presence of a curing agent. The cross-linking process for thermosets is very similar. In thermosets the polymer molecules are also chemically linked due to heat after processing.

Cross-linked rubbers have a wide-meshed molecular network that keeps them soft and their properties change only slightly on a wide temperature scale. On the other hand, thermosets are characterized by a very narrow-meshed network. Due to this fact they hardly change their high level of stiffness on a wide temperature scale.

The irradiation cross-linking of thermoplastic materials via electron beam or cobalt 60 (gamma rays) is proceeding separately after the processing. The cross-linking level can be adjusted by the irradiation dosage and often by means of a cross-linking booster (Fig. 1).

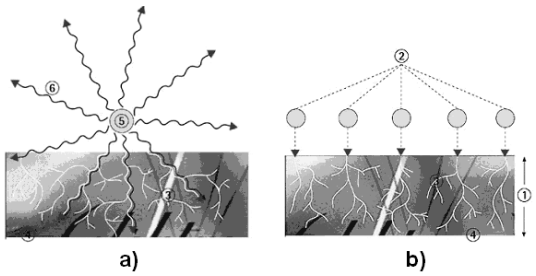

Fig. 1. **Design of Gamma rays (a) and Electron rays (b);** a) 3 – secondary electrons, 4 – irradiated material, 5 – encapsulated Co – 60 radiation source, 6 – Gamma rays, b) 1 – penetration depth of electron, 2 – primary electron, 3 – secondary electron, 4 – irradiated material

The main deference between beta and gamma rays lies in their different abilities of penetrating the irradiated material. Gamma rays have a high penetration capacity. The penetration capacity of electron rays depends on the energy of the accelerated electrons (Fig. 2).

Due to electron accelerators, the required dose can be applied within seconds, whereas several hours are required in the gamma radiation plant[1].

Cobalt 60 serves as the source of radiation in the gamma radiation plant. Many of these radiation sources are arranged in a frame in such a way that the radiation field is as uniform as possible. The products on pallets are conveyed trough the radiation field. The radiation dose is applied gradually, that is to say, in several stages, whereby the palleted products are conveyed around the Co – 60 radiation sources several times. This process also permits the application of different radiation doses from one product type to another. It can be used for irradiation of polyolefines, polyesters, halogen polymer and polyamides from thermoplastics group, elastomers and thermoplastic elastomers[2]. Some of them need the addition of crosslinking agent. The dimensional stability, strength, chemical resistance and wear of polymers can be improved by irradiation. Irradiation cross-linking normally creates higher strength as well as reduced creep under load if the application temperature is above the glass transition temperature (Tg) and below the former melting point[3]. Irradiation cross-linking leads to a huge improvement in resistance to most of the chemicals and it often leads to the improvement of the wear behaviour.

2. Experimental

Properties of unirradiated (natural) and irradiated TPE – E with the doses up to 199 kGy have been compared. Injection molding machine Arburg 420 C Allrounder Advance has been used for sample preparation[4,5]. Tested polymer: Thermoplastic elastomer TPE-E.

Tensile test has been carried out on the Zwick 1456 tensile testing machine according CSN EN ISO 527 - 1, 527 - 2 standard. Test Xpert standard software was used for test evaluation.Testing samples have been irradiated by the dose of 0, 66, 99, 132, 165 and 199 kGy.

3. Results and discussion

For easier and faster comparison of the measured values, so called dimensionless values ([-]) expressed as the ratio of separate measurements to the maximum value reached during the given measurements were used (Fig. 2 and Fig. 3).

3.1. Tensile strength, elongation

The dose of irradiation influence mechanical properties of monitored properties. The tensile strength is the highest with the dose of 66 kGy and with the higher dose falls of with the dose higher than 132 kGy oscillate tensile strength around the same value as in the case of not irradiated polymer.

The elongation is markedly influenced by irradiation. Higher dose of irradiation leads to important reduction of elongation. By the dose of 199 kGy is the reduction of elonga-

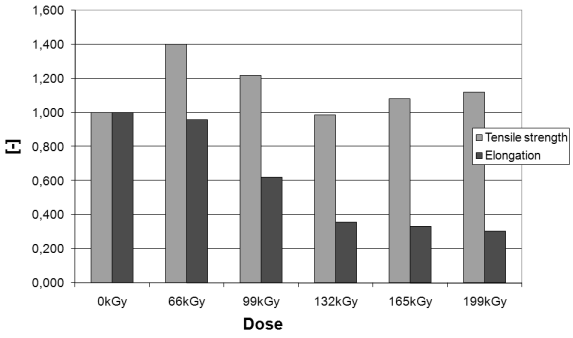

Fig. 2. **Comparison of tensile strength and elongation**

tion is four time in comparison with the unirradiated TPE-E (Fig. 2).

3.2. Modulus

Modulus of elasticity of irradiated thermoplastic elastomer TPE-E rises with the dose of irradiation. The highest difference between irradiated and unirradiated thermoplastic elastomer reached to 50 % with the dose of 199 kGy (Fig. 3).

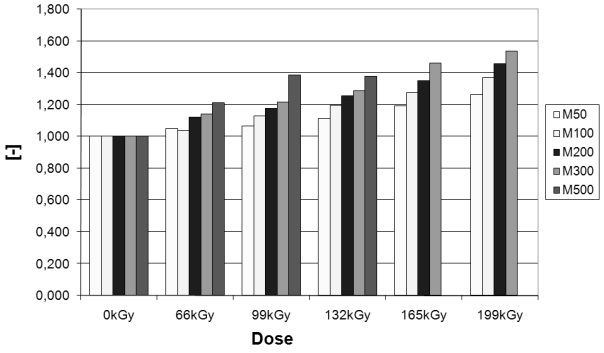

Fig. 3. **Comparison of modulus of elasticity**

4. Conclusion

The differences of mechanical properties of irradiated and natural thermoplastic elastomers TPE-E have been found out. Advantage of irradiation process laies in possibility to carry out the process on the final products, e.g. injection molded parts, extruded or thermoformed products. In other hand it is necessary to have in mind, that irradiation is and additional process which need additional cost. It is necessary to take in account all benefits/cost resulting from the irradiation process already during the design stage of the polymer part.

The energy of accelerated electrons effect the penetration ability of radiation.Thus only defined zone of the polymer product can be affected. The properties of polymer product would be controlled in this way.

This article is financially supported by the Czech Ministry of Education, Youth and Sports in the R&D project under the title 'Modelling and Control of Processing Procedures of Natural and Synthetic Polymers', No. MSM 7088352102 and 'CEBIA Tech', No. CZ.1.05/2.1.00/03.0089.

REFERENCES

1. Drobný J. G.: *Radiation Technology for Polymers*. CRC Press, Boca Raton 2003.
2. Crawford R. J.: *Plastic Engineering - 3 rd Edition*. Butterworth – Heinemann, Oxford 1998.
3. Dole M.: *The radiation chemistry of macromolecules*. Academic Press, New York and London 1972.
4. Stanek M., Manas M., Manas D., Sanda S.: Chem. Listy *103*, 91 (2009).
5. Stanek M., Manas M., Manas D.: *Mold Cavity Roughness vs. Flow of Polymer.* Novel Trends in Rheology III, AIP, New York, USA, p.75–85, (2009).

M. Maňas, D. Maňas, M. Staněk, Š. Šanda, and V. Pata *(Tomas Bata University in Zlin, Zlin, Czech Republic):* **Improvement of Mechanical Properties of TPE by Irradiation**

The article describes the effect of irradiation on properties of thermoplastic elastomer. The irradiation leads to huge improvement of their mechanical properties. The changes of properties depend on the dose of irradiation.The modulus of elasticity goes up to 50 % wheras the elongation drops to four times with the dose of irradiation of 196 kGy.